LEAD CHALCOGENIDE IR-EMITTERS AND DETECTORS ON Si-SUBSTRATES

H. Zogg, M. Arnold, D. Zimin, K. Alchalabi, K. Kellermann

Thin Film Physics Group, Swiss Federal Institute of Technology, Zurich, Switzerland

Abstract

Narrow gap IV-VI (lead chalcogenide) compounds are employed since long time as mid-IR-detectors and -lasers. IV-VIs are tolerant to structural defects (dislocations). This allows lattice mismatched MBE-growth on foreign substrates like Si which offers significant advantages with respect to size, costs and thermal conductivities.

In addition, IV-VIs are unique as regards design of Bragg mirrors because of the very high index contrast between IV-VI materials (n_H = 4-5) and BaF_2 (n_L=1.43). A few pairs of quarter wavelength n_H/n_L-stacks suffice to obtain very high reflectivities R>99%.

We review some of our results for different devices: Infrared sensor arrays for thermal imaging on active Si read-out chips, RCEDs (resonant cavity enhanced IR detectors), optically pumped PbSe/$Pb_{1-x}Eu_xSe$ edge emitting DH (double heterostructure) or QW (quantum well) lasers on Si substrates and “wavelength transformers”, VCSEL (vertical cavity surface emitting laser) structures operated in sub-threshold.

1. Introduction

Narrow gap lead chalcogenide (IV-VI) materials offer interesting applications for infrared detector arrays as well as infrared emitters in the 3- >12 µm wavelength range [1]. Since the materials are rather tolerant to defects, devices with reasonable properties may be grown even in layers containing a rather high density of threading dislocations. This allows to grow the layers by MBE (molecular beam epitaxy) even on lattice mismatched substrates like Si. Si-substrates are most interesting because of availability, costs and ruggedness, and because one may grow even on Si-chips which contain integrated electronics.

The lattice constants of the lead chalcogenide materials are 8-20% larger than those of Si. Many misfit dislocations form at the interface during growth leading to a considerable density of threading dislocations, which extend up to the surface. In addition, the thermal expansion coefficient of lead-chalcogenides is about 7 times higher than that of Si. Therefore, the high lattice and thermal mismatch strains have to relax. Fortunately, glide of dislocations in IV-VI materials is easy. The main glide planes are of {100} type, and the Burgers vectors <110>. The Schmid factors in (111) oriented layers are therefore different from zero, dislocations can glide in this main glide system under the influence of the thermal mismatch stress field to relieve strain. They glide on each temperature change [2,3]. In addition, two dislocations, which meet within a certain reaction distance may annihilate, or two dislocations may fuse so that one dislocation only is left [4]. Thermal cycling therefore leads to a reduction of the dislocation densities, no dislocation blocking occurs in IV-VI materials with the {100}<110> glide system. The dislocation densities may be determined directly by etch-pit counting, calculated from the X-ray diffraction rocking curve line widths, or from the low temperature saturation Hall mobilities (which are inversely proportional to the mean distance $1/\rho$ between two threading dislocations [ρ dislocation density]). The lowest dislocation densities we observed in about 10 µm thick layers were in the 10^6 cm^{-2} range. In thinner layers as used for IR-device fabrication dislocation densities are typically about 10^7 cm^{-2}. These rather high densities do not impede the fabrication of infrared sensors of acceptable quality: The high permittivities of IV-VI materials shield the electric fields caused by defects over short distances.

Below we review some of our results for different devices: Infrared sensor arrays for thermal imaging on active Si read-out chips, RCEDs (resonant cavity enhanced IR detectors), optically pumped $PbSe/Pb_{1-x}Eu_xSe$ edge emitting DH or QW lasers on Si-substrates and “wavelength transformers” (VCSEL (vertical cavity surface emitting laser) structures operated in sub-threshold).

Note that an additional essential advantage of using IV-VI materials for fabrication of RCEDs and VCSELs is that integrated Bragg mirrors can easily be fabricated. This is because of the very high index contrast between IV-VI materials (n_H = 4-5) and BaF_2 (n_L=1.43). A few pairs of quarter wavelength n_H/n_L-stacks suffice to get very high reflectivities R>99%.

2. MBE-Growth of Epitaxial IV-VI-on-Si Layers

The chalcogenide layers are grown by solid source molecular beam epitaxy (MBE) at temperatures between 250 °C and 450 °C. A 2-3 nm thick CaF_2 buffer layer is employed for compatibility [2,3]. This buffer layer is grown at up to 700°C if passive Si-substrates are used, or at 450°C on active Si-chips with Al-metallization. The preparation of the Si-substrate before MBE growth is crucial. For growth on passive Si(111), we use a modified Shiraki cleaning, where the artificially created surface oxide desorbs in the MBE growth chamber when heating immediately before growth to a temperature above 900°C. For growth on active Si-chips already containing an Al-metallization, a low temperature cleaning is employed. A H-terminated surface is created by etching with a HF/NH_4F mixture. N_2-bubbling ensures complete wetting [5]. When the sample is heated to the growth temperature, the H desorbs and the substrate is ready for deposition of the CaF_2, which forms a coherent layer. After the growth of the buffer layer, the sample is transferred in situ to the second growth chamber where the chalcogenides (and BaF_2 for the Bragg mirrors if needed) are deposited. The layers exhibit smooth surfaces except the slip lines due to the dislocation glide, which has occured to relieve the lattice- and thermal expansion mismatch.

3. Infrared Sensor Arrays for Thermal Imaging on Active Si Read-Out Chips

Infrared focal plane arrays (IRFPA) for thermal imaging fabricated with direct band narrow gap semiconductors (NGS) offer the highest sensitivities at a given operation temperature, and integration times can be short due to their high sensitivities and fast response. The signal read-out of the numerous pixels in large 2-d arrays is preferentially performed in Si-technology. This leads to the present hybrid NGS-Si IRFPA lay-outs with e.g. InSb or HgCdTe as sensor material [1]: The NGS chip with the sensor pixels is mated to the Si read-out integrated circuit (ROIC) with In-bumps or loop-holes.

Considerable simplifications and cost savings would result if the NGS layer could be grown directly onto the Si-ROIC chip, thus leading to a heteroepitaxial, but monolithic IRFPA. However, the high structural quality of the NGS layers needed might not easy be attained due to the large lattice and thermal expansion mismatch of the known NGS materials with respect to Si.

IV-VI semiconductors (lead chalcogenides) are much easier to grow and handle than

HgCdTe. They are "forgiving", i.e. layers with much lower structural quality suffice to get useful devices while the theoretical performance of NGS IV-VIs is the same as HgCdTe under similar conditions. We realized 1-d photovoltaic PbSnSe LWIR (8-12 µm wavelength range) and MWIR (3-5 µm) PbTe arrays on Si(111) already some time ago, as well as $Pb_{1-x}Eu_xSe$ arrays for the SWIR (2-4 µm) range [1,3].

Fig. 1 shows part of a 2-d IRFPA grown on an active Si-substrate which contains read-out electronics, and Fig. 2 a schematic cross-section of a pixel [5]. The photovoltaic IR-detector is formed by a p-PbTe/Pb semiconductor/metal junction. The size of the array is 96 x 128 pixels on a 75 µm pitch. Each pixel on the Si(111) substrate contains a switching transistor and a bare area where epitaxial growth of the IV-VI material occurs during MBE-deposition. Arrays are then processed with photolithographic techniques.

In well processed arrays, >97% of the pixels are working and, as usual for NGS devices, high external quantum efficiencies (~60%) are observed. The sensitivities were obtained by measuring the differential resistances Ro at zero bias and normalized with the area A of a device. The mean resistance area product RoA is about 90 Ωcm^2 at 95K operating temperature. This is >10 times above the background noise limit (BNL) for room temperature (RT) radiation and 180° field of view [6]. The chips were employed to set-up a demonstrational thermal imaging camera.

4. Resonant Cavity Enhanced IR Detectors (RCEDs)

The detectors described above exhibit a flat spectral response up to the cut-off wavelength. If a narrow band spectral sensitivity is desired, the active detector material may be placed inside a cavity. The Q-factor of the cavity is determined by the reflectances of the two end-mirrors, and the absorption of the active detector part. Very high Q-factors leading to very narrow spectral sensitivity may be obtained. In addition, despite a very thin detector layer, quantum efficiencies approaching 1 are obtained since a photon at the resonance wavelength is reflected back and forth many times within the cavity before it is absorbed. Since the detector volume is small, in addition, higher sensitivities than with optimized bulk-detectors result.

Fig. 3 shows the structure we realized [7]. The radiation impinges through the Si-substrate. The bottom Bragg mirror consists of two $Pb_{1-x}Eu_xSe/BaF_2$ pairs. The Eu composition x=0.5 is chosen in order that it does not absorb at the design wavelength λ_o=4.4 µm. The calculated reflectivity of the mirror at λ_o is 94 %. The optical thickness of the cavity is designed for 5th order at λ_o. The thicker bottom part again consists of about 3 µm $Pb_{1-x}Eu_xSe$, nonabsorbing at λ_o. The thin top part terminating the cavity is the active detector absorbing layer, $Pb_{1-y}Eu_ySe$ (y<x) with y=0.3. The corresponding cut-off wavelength is somewhat larger than λ_o. This ensures highest sensitivity at as high as possible operating temperature, and, in addition, lower order modes (with higher wavelengths) are not sensed. The top mirror is metallic Pb. Pb forms a blocking contact with IV-VI materials, thus resulting in a photovoltaic IR-detector as in the case of the arrays described in the previous section. The ohmic contact is formed by electrodeposited Au.

The measured spectral quantum efficiency is plotted in Fig. 4. Only the line with order m=5 is visible. Its linewidth (FWHM) is as narrow as $\Delta\lambda$ = 0.035 µm ($\Delta\lambda/\lambda_o$ = 0.8%), and the peak quantum efficiency as high as 32%. This is obtained without AR-coating of the Si substrate. With AR-coating, the value would increase to 45 %. The sensitivities we obtained so far with such detectors are above the BNL for operation temperatures up to about 150K.

5. Optically Pumped PbSe/$Pb_{1-x}Eu_xSe$ Edge Emitting DH or QW Lasers on Si Substrates

Optically pumped PbSnSeTe lasers on IV-VI substrates were already described [8]. With the introduction of compact high-power laser diodes emitting in the 800 - 1600 nm wavelength range, low-cost optically pumped lead chalcogenide IR-emitters for wavelengths above 3 µm become attractive. With optical pumping, no p-n junctions with low ohmic contacts have to be fabricated as for electrically pumped sources, and the design freedom is higher. This includes use of high resistance cladding layers like $Pb_{1-x}Eu_xSe$ with larger Eu-content and lower carrier concentrations (which in addition diminishes Auger recombination).

The structure of the QW edge emitting laser of Fig. 5 consists of a bottom $Pb_{1-x}Eu_xSe$ cladding layer, the active $Pb_{1-y}Eu_ySe$ (y<x) layer containing three PbSe quantum wells (QW), and a top EuSe cladding layer which is transparent to the incoming pump beam. This structure is grown on a (100)-oriented Si wafer precovered with an epitaxial CaF_2/BaF_2 buffer layer [8]. The 2-3 µm thick IV-VI stack is (100) oriented. Since the Si-substrate does not cleave along (100) as the IV-VIs do, the IV-VI epitaxial layer is lifted off from the substrate by dissolving the BaF_2 buffer in water, cleaved into a rectangle with a few mm long and a 300 µm short side length. It is clamped between a heat-conducting substrate and a glass cover transparent to the pump beam. The pump beam is focussed across the short length of the rectangle using a lens, thus forming a gain-guided structure with a cavity length L=300 µm.
A pulsed III-V laser diode with 870 nm emission wavelength and a maximum peak pump power of 5.5 W_p at the sample was used as pump source. The light-out vs light-in characteristics for the QW structure of Fig. 5 is shown in Fig. 6 for different temperatures. Output power is up to 200 mW with this restricted pump power, and differential quantum efficiency is as high as 20%. The laser emission is multi-mode. The highest heat sink temperature where lasing is observed is about 240K (restricted by the power of the pump laser).

IV-VI layers with (111) orientation grown on Si(111) substrates are of higher structural quality [3]. Here, thermal mismatch strains relax on each temperature cycle. Since the cleavage planes of IV-VIs are of {100}-type, the cavity mirrors have to be etched for (111)-oriented layers. We developed a dry processing technology which yields smooth vertical mirror faces. The back mirror is just a quarterwave air ($\lambda/4$) groove which yields a (calculated) reflectivity of 78% (Fig. 7). There is no need for epitaxial lift-off with this technique. Double hetero (DH) laser structures were fabricated. The threshold intensity as a function of temperature of such a structure is shown in Fig. 8. The threshold remains essentially constant up to 200K, then it increases. Lasing (employing again the 5.5 W_p pump diode-laser) was observed up to 250K heat sink temperature.

Nearly similar results, but with somewhat still lower threshold pump intensities at low temperatures are observed when the structures are grown on $BaF_2(111)$ substrates (second curve in Fig. 8). With this substrate, thermal expansion mismatch is absent since the thermal expansion coefficients of BaF_2 and IV-VI materials are almost equal.

These characteristics are compared with calculated threshold intensities for DH-structures. It turns out that the measured thresholds are up to more than two ordes of magnitude higher than the calculated ones, the latter being due to the fundamental Auger recombination and spontaneous emission. The results are roughly explained by assuming a Shockley-Read lifetime as short as 0.1 ns which is caused by the high threading dislocation density $> 10^8$ cm^{-2} in these structures [9]. Since our present technique allows fabrication of IV-VI-on-Si structures with dislocation densities $< 10^7$ cm^{-2}, there is ample room to still increase material quality of the present laser structures to obtain higher S-R lifetimes. This will lead to considerably lower threshold intensities, or operation to higher temperatures even with the restricted emission powers of the pump diodes we employed.

6. "Wavelength transformers", VCSEL structures operated in sub-threshold.

In general, photoluminescence is broadband and extends over a wide emission angle. In order to obtain a narrow, peaked emission line, resonant cavity structures may be designed. In our device (Fig. 9), the $Pb_{1-x}Eu_xSe$ active layer contains PbSe QWs (each 20 nm thick) at the antinodes of the standing wave and has an optical thickness of $\lambda/2$ where λ is the center wavelength of the emission line. It is sandwiched between two integrated Bragg mirrors. The bottom (epitaxial) mirror consists of a single $BaF_2/Pb_{.95}Eu_{.05}Se$ L/H pair where each layer has $\lambda/4$ optical thickness. The low index L is 1.43 (BaF_2), the high index H is about 4.5 ($Pb_{.95}Eu_{.05}Se$). Note that already one or a few HL-pairs yield high reflectivity R due to the high index contrasts. (R is already 88% for one single L/H pair). The active layer on the bottom mirror is overgrown with the top mirror pairs. Here, we used three BaF_2/EuSe $\lambda/4$ pairs (high refractive index h=2.4 for EuSe). This mirror is transparent to the incoming light beam of the III-V laser diode, and its reflectivity at 4.2 µm is 97%. Alternatively, since this mirror must not consist of an epitaxial material, polycrystalline SiO_2/TiO_2 L/H pairs may be evaporated or sputtered in a separate system. Both combinations exhibit nearly the same refractive indices. We tried both variants with equal success.

The device (its structure exactly corresponds to a VCSEL, but with lower reflectivity end mirrors) is operated at RT in the subthreshold region. Its line width is about 6% for the present realisation, and power efficiency is above 10^{-4}. By changing the mirror reflectivities, the quality-factor of the whole structure may be tuned [10]. The position of the gain curve is determined by the well width and allows optimization for narrow band emission ranging from about 3 to 4.6 µm at RT. This allows easy tuning to the absorption lines of gases like CO_2, CO or CH_4. The Si substrate is transparent to the output beam and also acts as a mechanical protection. This is at variance to its II-VI counterpart, where an expensive CdZnTe-substrate and lift-off techniques had to be employed [11].

Note that optically pumped IV-VI VCSELs taking advantage of the high index contrast with IV-VI materials have already been described by two groups [12,13]. These structures were grown on BaF_2 substrates, and pulsed laser emission up to RT was achieved. However, large laboratory type pump lasers were used for excitation.

7. Conclusions

Although IV-VI materials are not on the mainstream of present optoelectronic IR-devices, the unique properties of IV-VIs allow to obtain useful devices with quite a limited effort. In the present review, the following IV-VI optoelectronic devices fabricated in layers grown by MBE on Si-substrates have been described:

- monolithic heteroepitaxial IR-FPA on active Si-substrates,
- resonant cavity infrared detectors (RCED) with spectral linewidths as narrow as 0.8%,
- optically pumped edge emitting mid-IR lasers, and
- "wavelength transformers", VCSELs operating in the subthreshold region.

These devices demonstrate a broad application range of the narrow-gap IV-VI materials as detectors for thermal imaging and hyperspectral spectroscopic applications as well as emitters for various gas sensing spectroscopies.

Corresponding author: Hans Zogg, Thin Film Physics Group, Swiss Federal Institute of Technology, Technoparkstr. 1, CH-8005 Zurich, Switzerland, phone +41 1 445 1480, fax +41 1 445 1499, zogg@phys.ethz.ch, http://www.tfp.ethz.ch

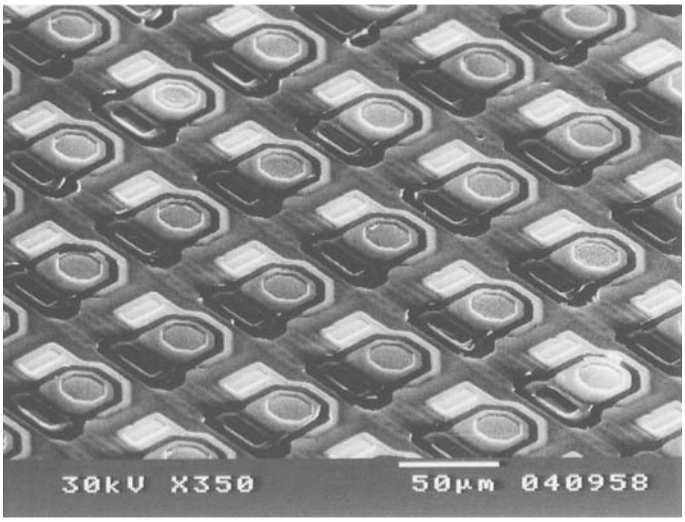

Fig. 1. Part of the completely processed monolithic 96 x 128 PbTe-on-Si IR-FPA for the MWIR with the read-out electronics in the Si-substrate.

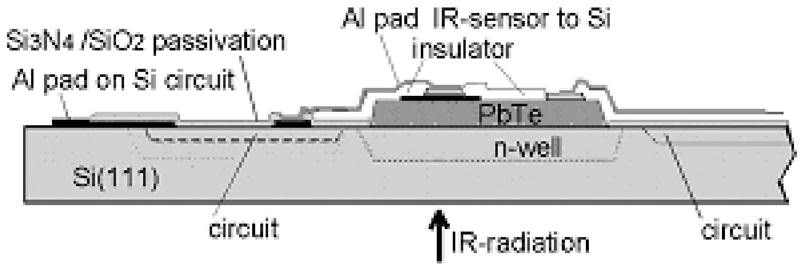

Fig. 2. Schematic cross-section of one pixel with the PbTe island as backside illuminated photovoltaic IR-sensor, and the electrical connections to the Si circuit (access transistor) and common anode.

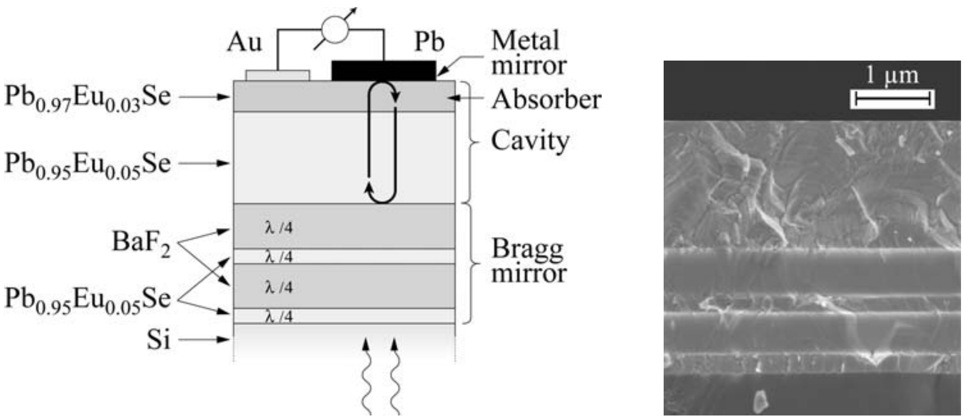

Fig. 3. Schematic cross section of a resonant cavity enhanced IR-photodetector realized with IV-VI materials on a Si substrate, and scanning electron micrograph of a cleaved cross section of the device.

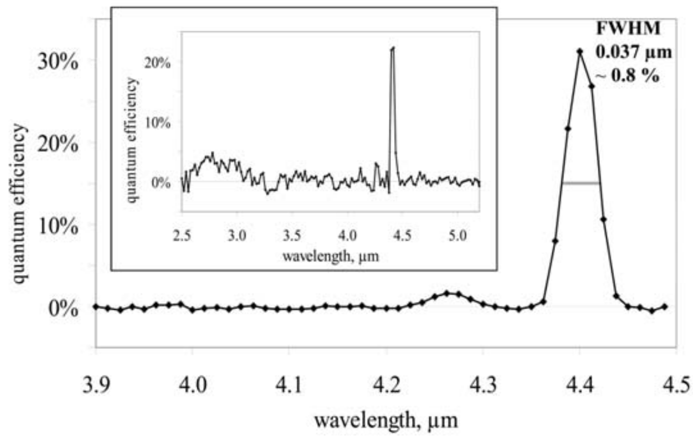

Fig. 4. Spectral quantum efficiency of the narrow band resonant cavity detector (RCED) with 32% peak efficiency (without AR-coating).

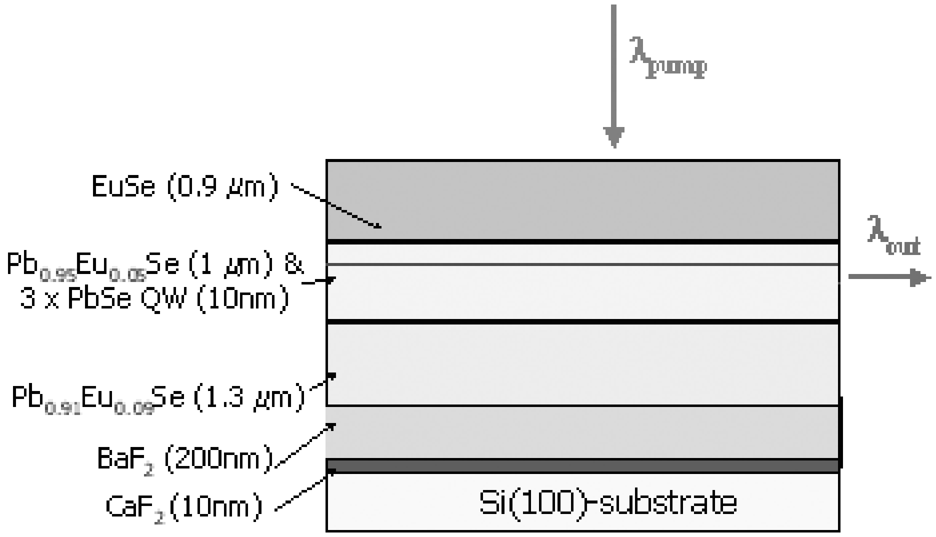

Fig. 5. Structure of an optically pumped QW IV-VI laser on a Si(100)-substrate.

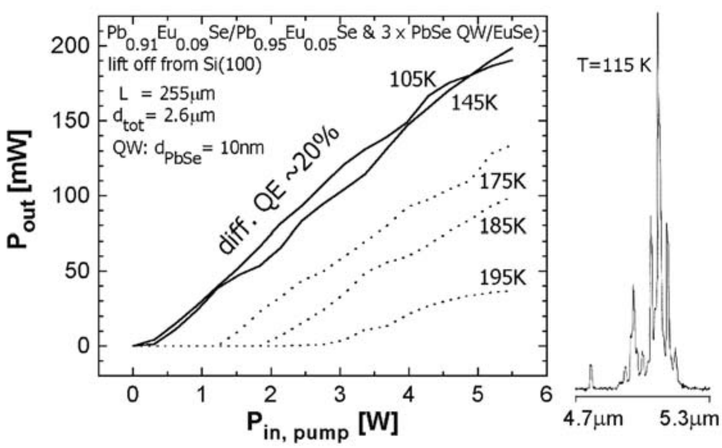

Fig. 6. Light-in/light-out characteristics of the laser structure of Fig. 5 (lifted off from the temporary (100) Si-substrate), and laser spectrum at 115K.

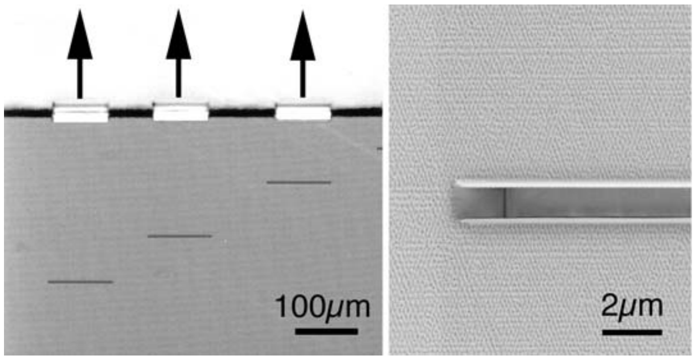

Fig. 7. FIB (focussed ion beam) etched mirrors in a IV-VI on Si(111) DH laser structure containing 3 different cavity lengths (left) and enlarged detail (right).

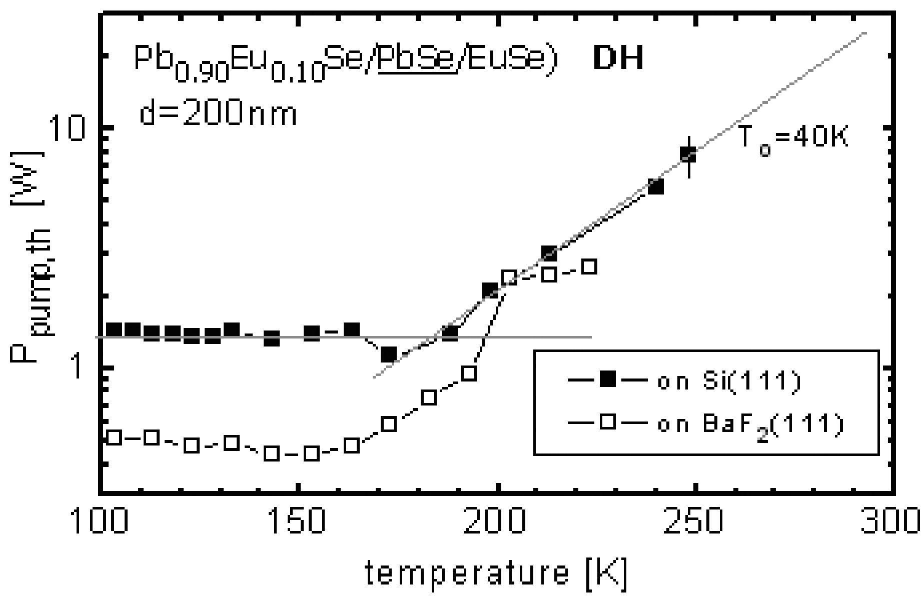

Fig. 8. Threshold pump powers vs T for a (111) oriented layer grown on Si(111) with etched mirror faces. For comparison, the results of a similar structure, but grown on a BaF_2 substrate, are indicated, too.

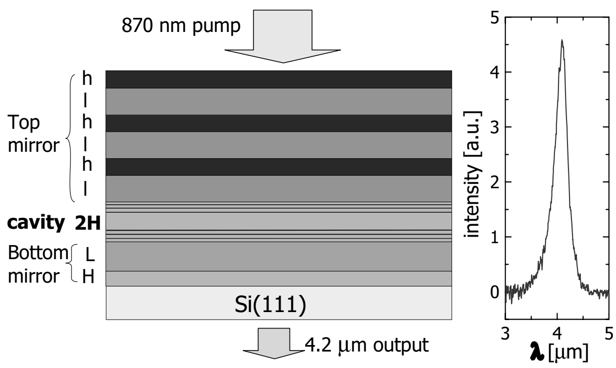

Fig. 9. Structure of a resonant cavity mid-IR source for optical excitation and corresponding emission spectrum at RT. The active cavity consists of 6 PbSe QWs embedded in a $Pb_{1-x}Eu_xSe$ layer and is sandwiched between two Bragg mirrors.

References

[1] H. Zogg, A. Ishida, IV-VI (lead chalcogenide) infrared sensors and lasers, in Infrared Detectors and Emitters, P. Capper, C.T. Elliott, eds., Kluwer Acad Publ 2000.

[2] G. Springholz, Z. Shi, H. Zogg, in "Heteroepitaxy: Thin Film Systems", Eds. W.K. Liu and M.B. Santos, Ch. 14, pp. 621-688, (World Scientific Publishing, Singapore, 1999)

[3] H. Zogg,"Lead Chalcogenide Infrared Detectors Grown on Silicon Substrates", in "Optoelectronic Properties of Semiconductors and Superlattices", M.O. Manasreh, Series editor, Vol. 18, "Lead Chalcogenides: Physics and Applications", D. Khokhlov ed., Taylor & Francis Books, Inc., New York and London, pp 587-616, 2003.

[4] P. Müller, H. Zogg, A. Fach, J. John, C. Paglino, A.N. Tiwari, M. Krejci, and G. Kostorz "Reduction of threading dislocation densities in heavily lattice mismatched PbSe on Si(111) by glide" *Phys. Rev. Lett.*, vol. 78, pp. 3007-3010, 1997.

[5] H. Zogg, K. Alchalabi, D. Zimin, Klaus Kellermann, Two-dimensional monolithic lead chalcogenide infrared sensor arrays on silicon read-out chips and noise mechanisms, IEEE Trans. Electron Devices ED50, pp. 209 - 214, Jan 2003.

[6] State of the art *hybrid* NGS IRFPA exhibit still much higher values, however.

[7] M. Arnold, D. Zimin, K. Alchalabi, H. Zogg, in preparation

[8] D.M. Dureev, O.I. Davarashivili, I.I. Zasavitskii, B.M. Matsonashvili, A.P. Shotov, Optically pumped $Pb_{1-x}Sn_xSe_{1-y}Te_y$ heterojunction lasers with matched gratings at the interface, Soviet-Journal-of-Quantum-Electronics. Dec. 1978, 8(12), 1481-3 (Original: Kvantovaya-Elektronika,-Moskva. Dec. 1978, 5(12), 2630-3)

[9] K. Kellermann, D. Zimin, K. Alchalabi, H. Zogg, Optically pumped lead-chalcogenide mid-infrared lasers on Si-substrates, J. Appl. Phys. 94, 7053, 2003.

[10] H. Zogg, K. Kellermann, K. Alchalabi, D. Zimin, Optically pumped lead-chalcogenide mid-infrared emitters on Si-substrates, Infrared Phys. Technol., in print

[11] E. Hadji, E. Picard, C. Roux, E. Molva, P. Ferret, 3.3 um microcavity light emitter for gas detection, Optics Lett. 25, 725, 2000.

[12] W. Heiss, T. Schwarzl, G. Springholz, K. Biermann, K. Reimann, "Above room temperature mid-infrared lasing from vertical cavity surface emitting PbTe quantum well lasers", Appl. Phys. Lett. 78, 862, 2001.

[13] F. Zhao, H. Wu, Lalith Jayasinghe, Z. Shi, Above room temperature optically pumped 4.12 um midinfrared vertical cavity surface emitting lasers, Appl. Phys. Lett. 80, 1129, 2002.